GW Open Data Workshop
April 18-20, 2024

Continuous Gravitational Waves

Takahiro S. Yamamoto (RESCEU U. Tokyo, Japan)

GW Open Data Workshop #7, April 18-20, 2024 @ Taichung, Taiwan

Introduction

Various types of GWs

Fig: https://spaceaustralia.com/news/cosmic-lighthouses-and-continuous-gravitational-waves credit: Shanika Galaudage

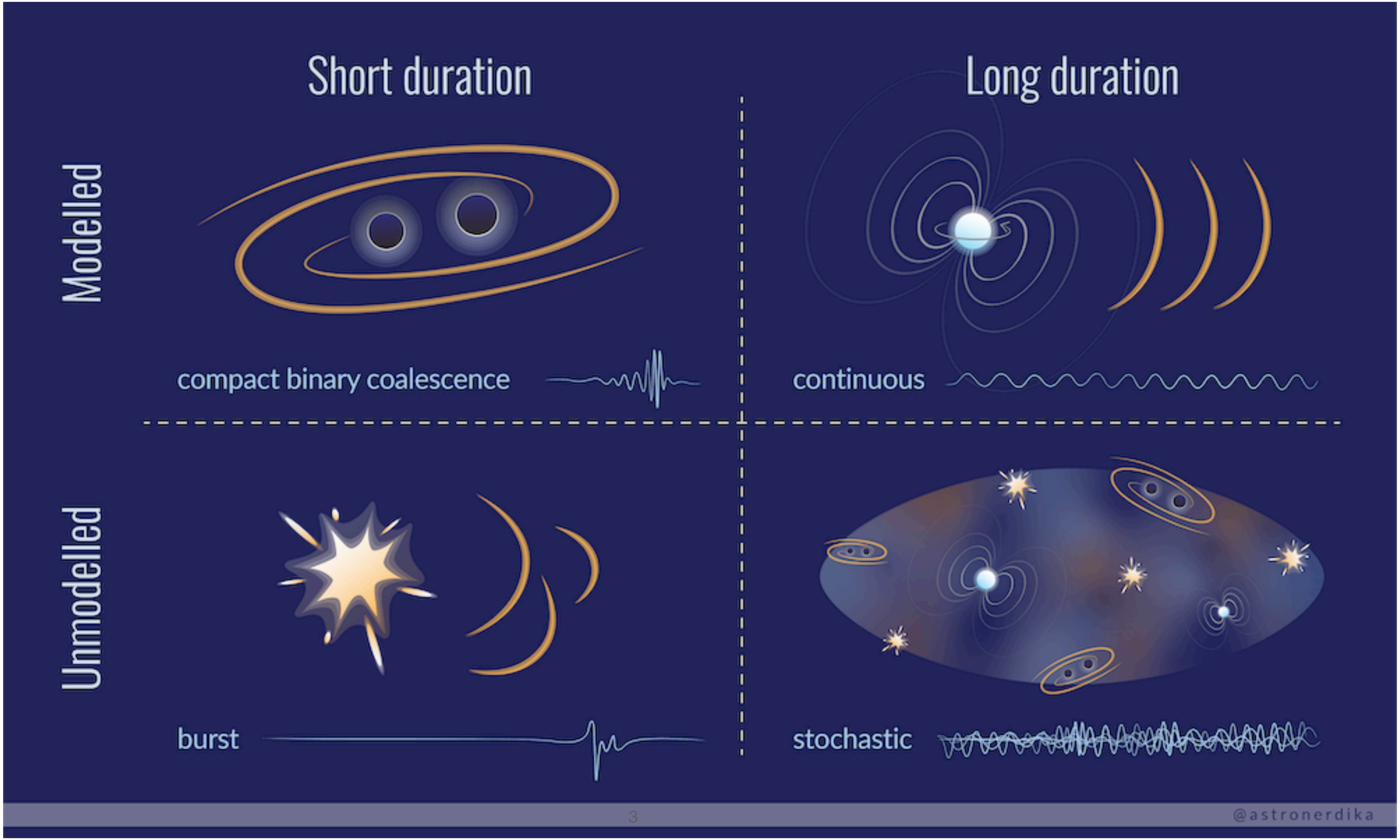

Fig: https://spaceaustralia.com/news/cosmic-lighthouses-and-continuous-gravitational-waves credit: Shanika Galaudage

Various types of GWs

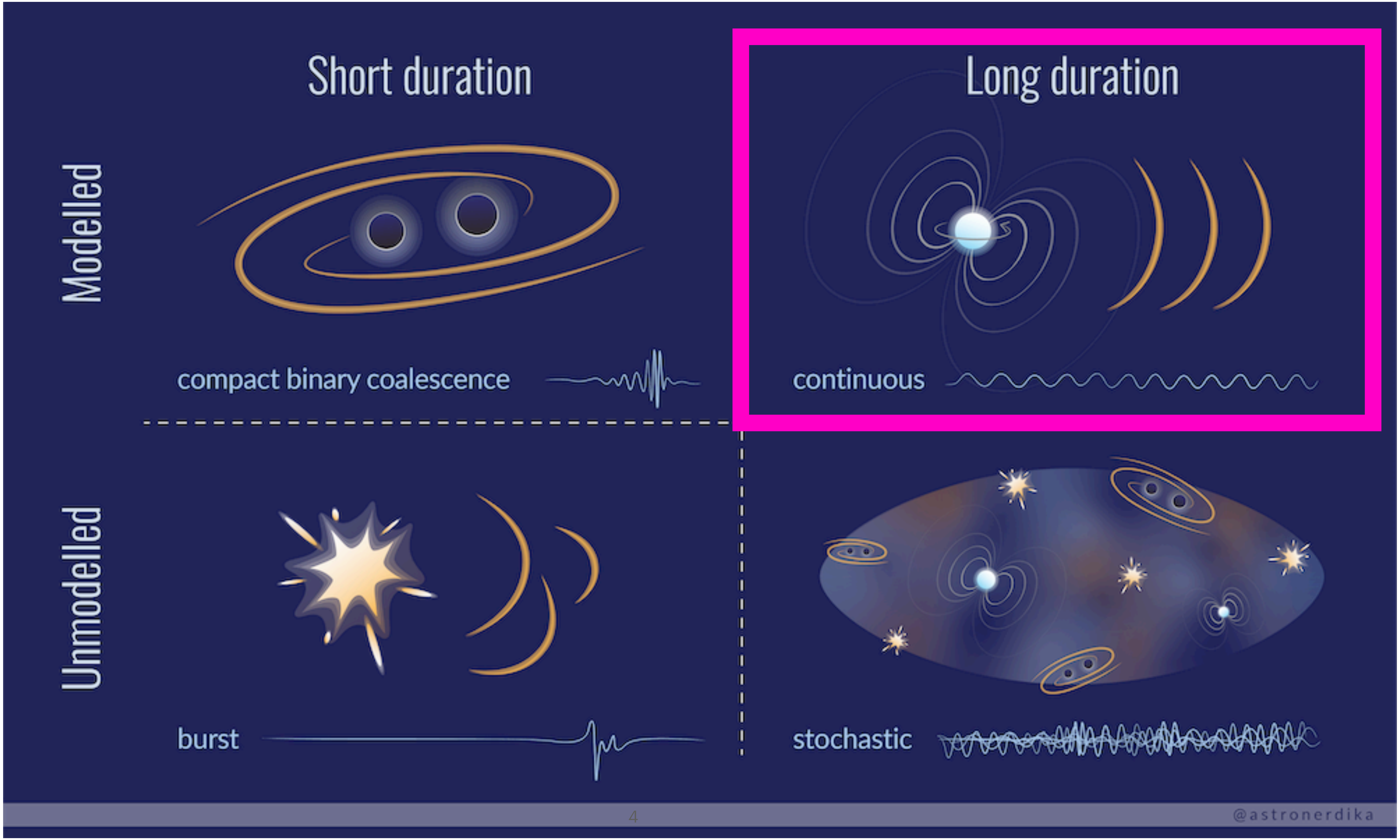

Sources of CGWs for ground based detectors

Rotating, distorted neutron stars (pulsars)

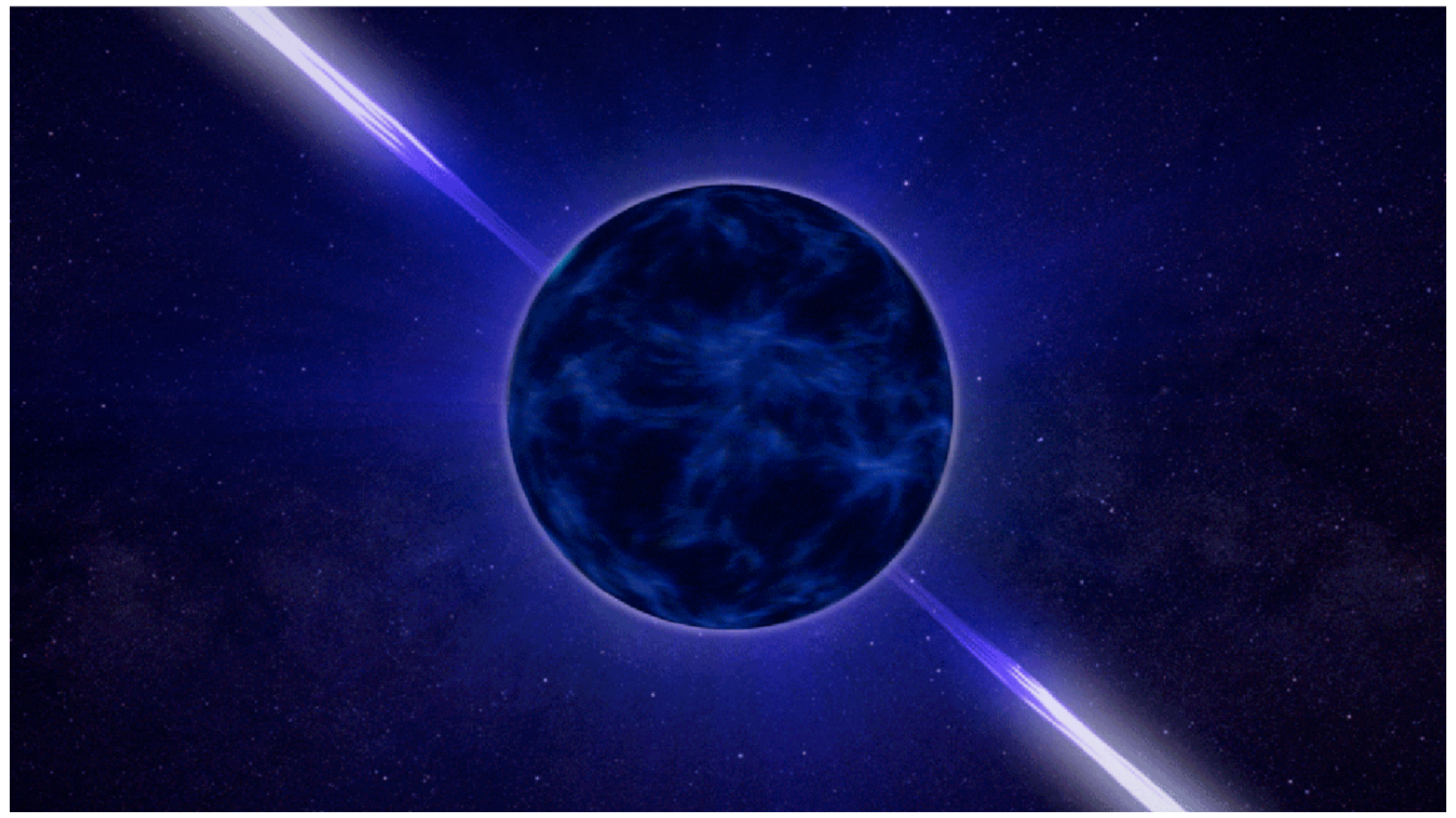

An artist's impression of a pulsar/neutron star.
Credits: NASA's Goddard Space Flight Center

→ **Astrophysics, nuclear physics**

Boson cloud around rotating BHs

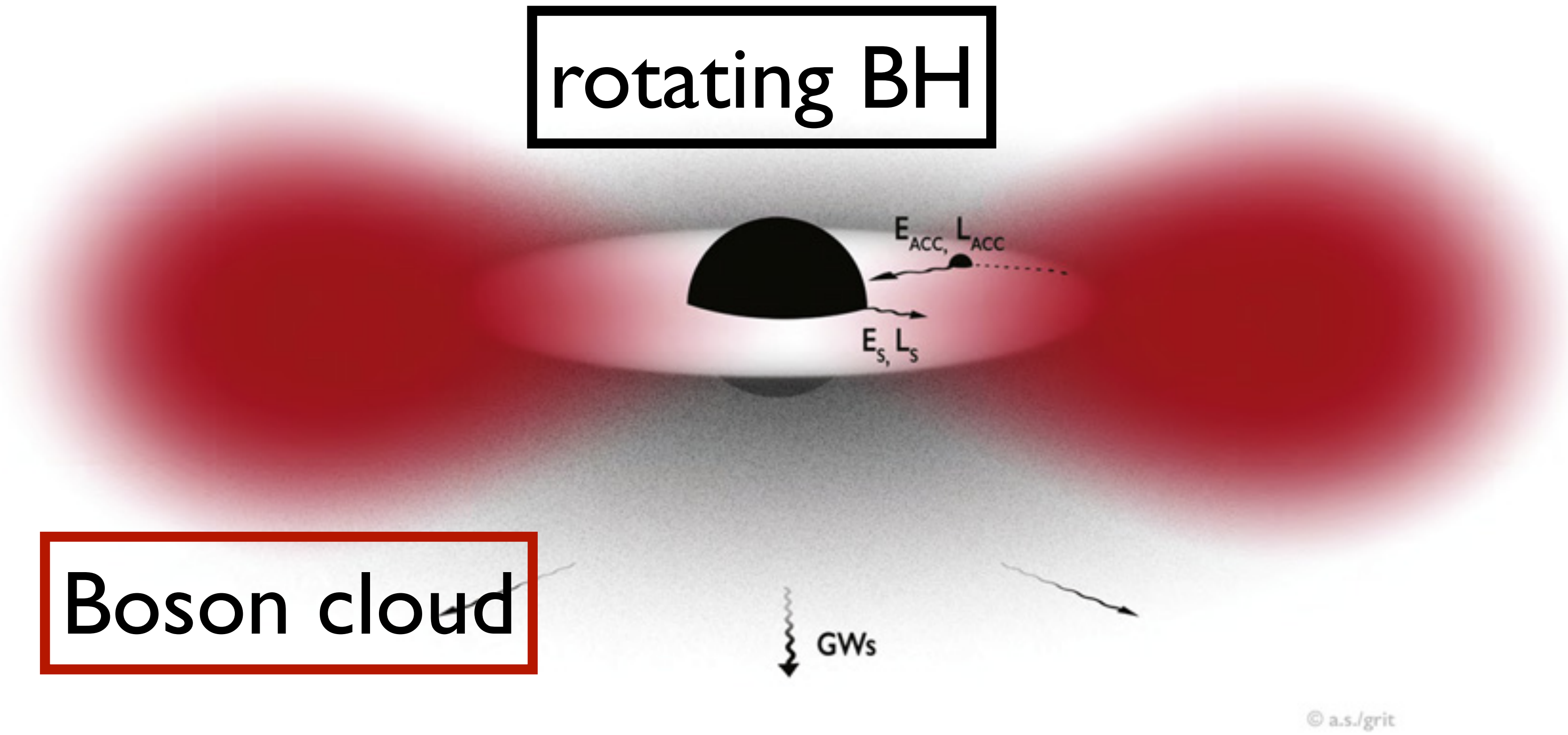

Arvanitaki *et al.*, PRD 81, 123530 (2010)
Brito *et al.*, Class. Quantum Grav. 32, 134001 (2015)

→ **Particle physics**

Planetary mass primordial BHs (cosmological origin)

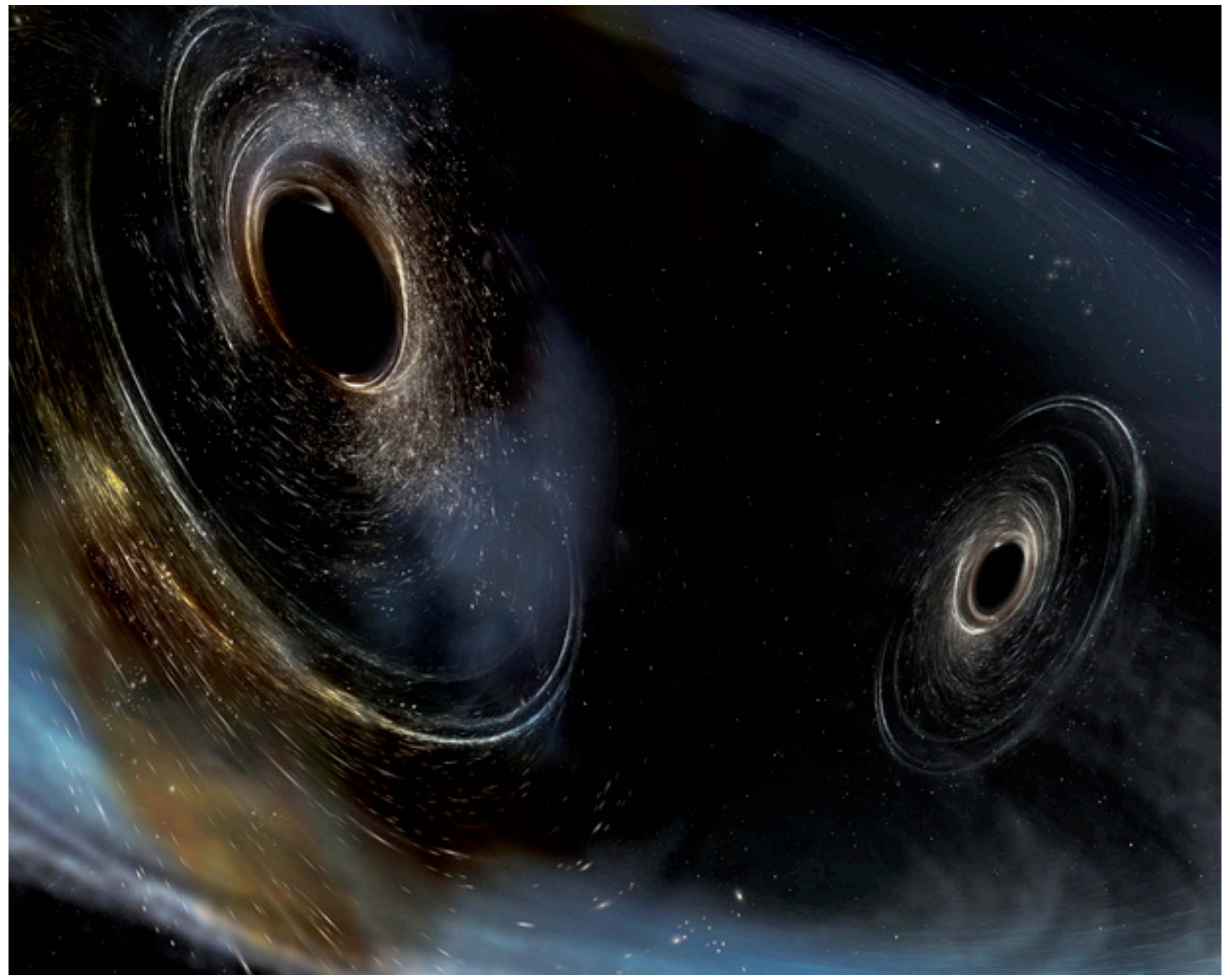

Sasaki *et al.*, Class. Quantum Grav. 35, 063001 (2018) as a review of PBH

→ **Cosmology**

Continuous gravitational waves (CGWs)

- **Persistent, quasi-monochromatic** signals
- Amplitude is **very weak**.
  - e.g. spinnig deformed NS

$$h_0 = \frac{4\pi^2 G}{c^4}\frac{I_3 f_{GW}^2 \epsilon}{d} = 4.2\times 10^{-26}\left(\frac{\epsilon}{10^{-6}}\right)\left(\frac{P}{10\ \mathrm{ms}}\right)^{-2}\left(\frac{d}{1\ \mathrm{kpc}}\right)^{-1}$$

ε : ellipticity, P : pulse period, d : distance

- We need to accumulate O(yr)-long strain data to detect CGWs.
- We have not detected CGWs yet.

Constraint from LIGO-Virgo O3 data

Fig. LVK collaboration, arXiv:2201.00697

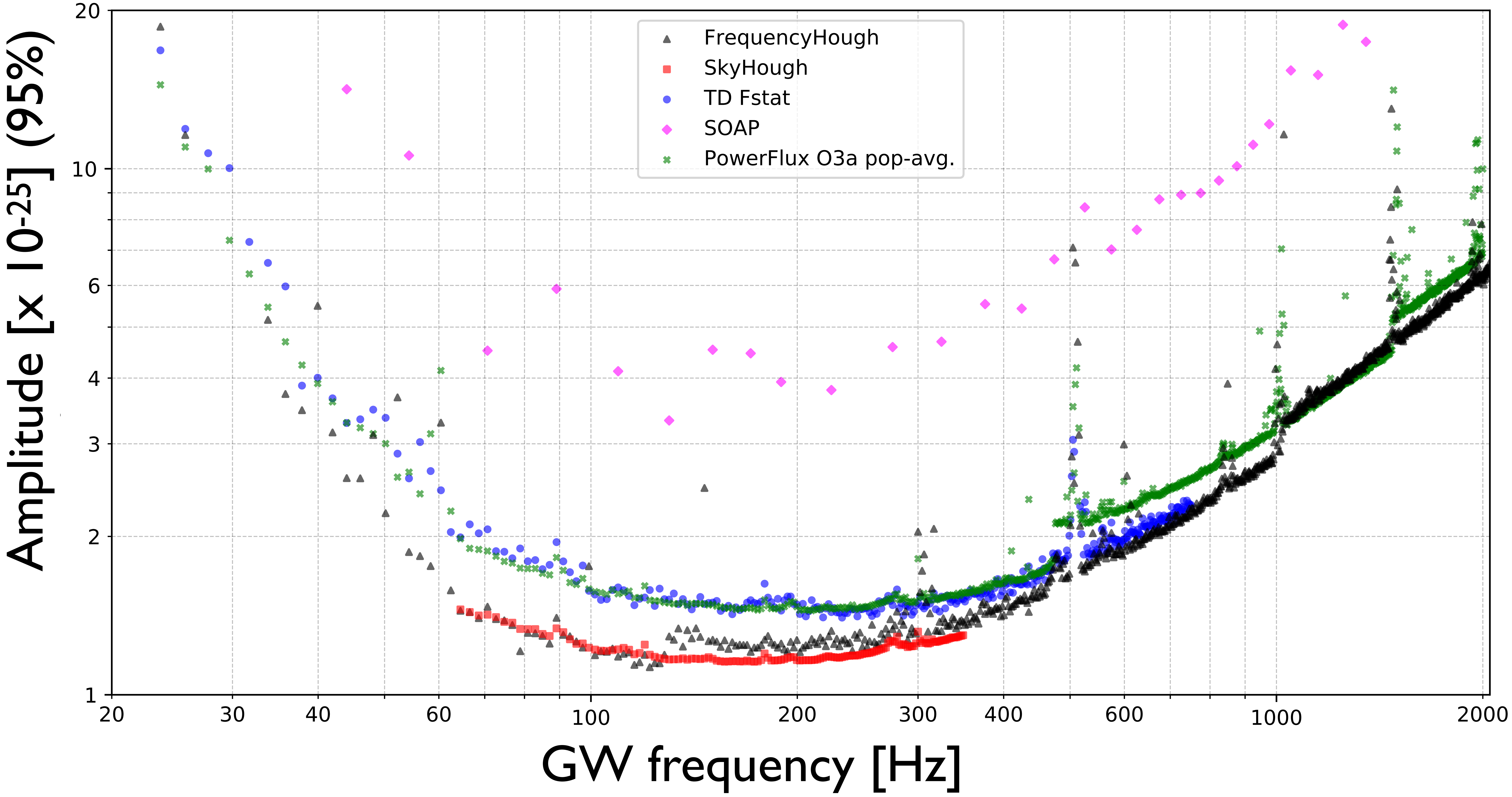

Waveform model of CGWs

in source frame

τ : time when wavefront reaches at SSB (solar system barycenter)

Two polarizaion of GWs $h_+(\tau) = h_0 \cos[\Phi(\tau) + \Phi_0], h_\times(\tau) = h_0 \sin[\Phi(\tau) + \Phi_0]$

Phase of GWs $$\Phi(\tau) = 2\pi \sum_{k=0}^{s} \frac{f^{(k)}}{(k+1)!} (\tau - \tau_{\rm ref})^{k+1}$$

Frequency parameters $$f^{(k)} := \frac{d^k f}{d\tau^k}$$

At emission, the model of CGWs is simpler than those of CBCs.

Detector motion makes it complicated.

Waveform model of CGWs

in detector frame

1. Inclination angle

Amplitudes of +, x modes $$h_+ \to h_0 \frac{1+\cos^2\iota}{2},\ h_\times \to h_0 \cos\iota$$

2. Detector's antenna patterns

$$F_+(t;\alpha,\delta,\psi) = \sin\zeta\left[a(t;\alpha,\delta)\cos(2\psi) + b(t;\alpha,\delta)\sin(2\psi)\right]$$
$$F_\times(t;\alpha,\delta,\psi) = \sin\zeta\left[b(t;\alpha,\delta)\cos(2\psi) - a(t;\alpha,\delta)\sin(2\psi)\right]$$

ψ : polarization

ζ : Angle btw arms, π / 2 for LVK

3. Doppler modulation due to the detector motion

$$\tau = t - \frac{\boldsymbol{r}(t)\cdot\boldsymbol{n}(\alpha,\delta)}{c}$$

τ : SSB time, t : detector time

$\boldsymbol{r}(t)$: detector location with respect to SSB

$\boldsymbol{n}(\alpha, \delta)$: unit vector pointing from SSB to the source

What we will observe is

$$h(t) = F_+(t;\alpha,\delta,\psi)h_0\frac{1+\cos^2\iota}{2}\cos\left[\Phi(t)+\Phi_0\right] + F_\times(t;\alpha,\delta,\psi)h_0\cos\iota\sin\left[\Phi(t)+\Phi_0\right]$$

Frequency modulation

$$\Phi(\tau) = 2\pi \sum_{k=0}^{s} \frac{f^{(k)}}{(k+1)!} (\tau - \tau_{\mathrm{ref}})^{k+1}$$

$$\tau = t - \frac{\boldsymbol{r}(t) \cdot \boldsymbol{n}(\alpha, \delta)}{c}$$

$$\begin{aligned} f(t) &= \frac{1}{2\pi} \frac{d\Phi}{dt} \\ &\sim (f^{(0)} + f^{(1)} t + \cdots) \times \left(1 + \frac{\boldsymbol{r}(t) \cdot \boldsymbol{n}}{c}\right) \\ &\sim \text{daily oscillation} + \text{yearly oscillation} + \text{intrinsic evolution} \end{aligned}$$

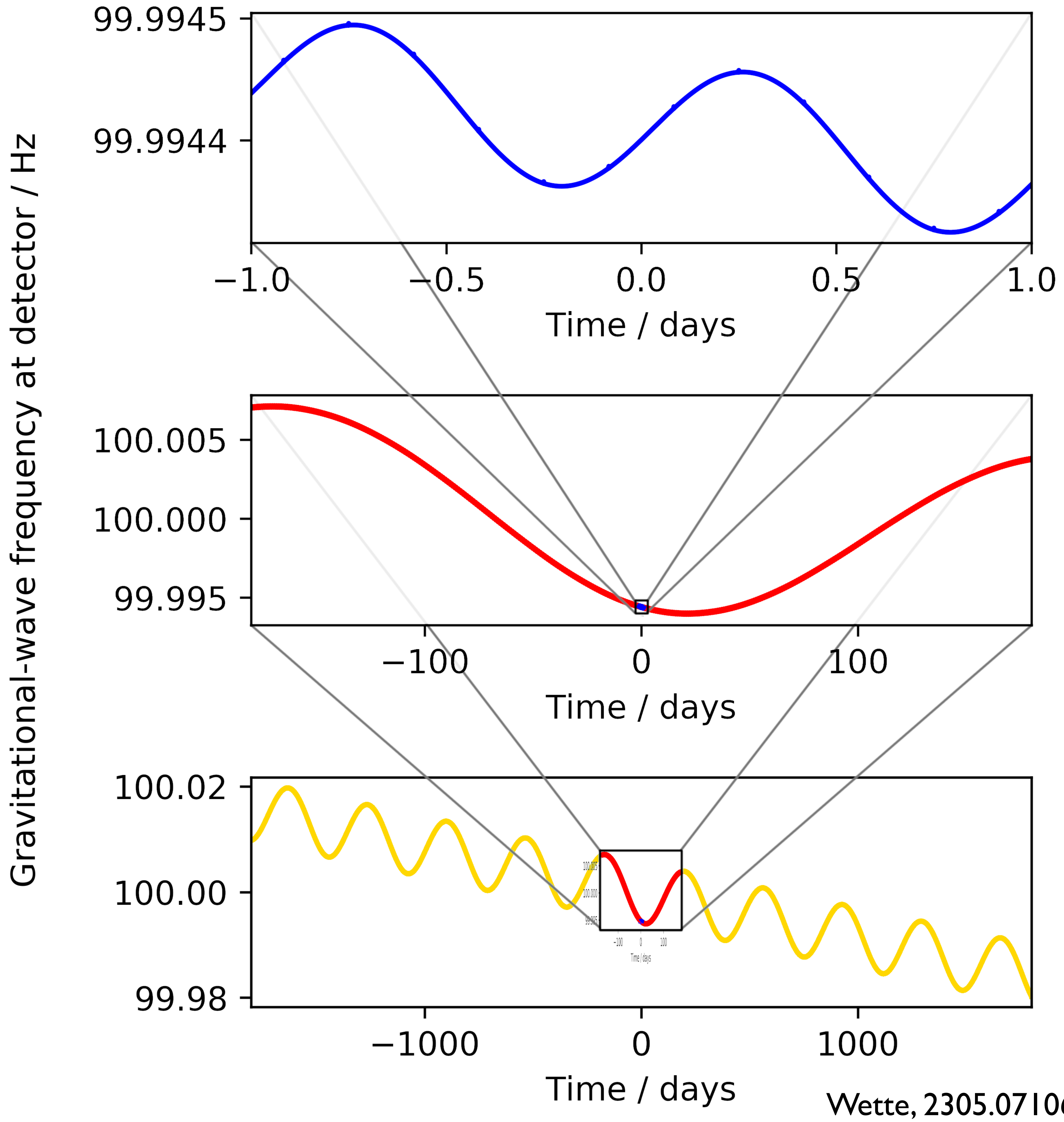

Wette, 2305.07106

Difficulties in CGW searches

- **Non-Gaussian detector noise**

  There are two types of non-Gaussian detector noise; glitches and lines. They can affect the sensitivity by increasing the false-alarm rate and elevating the noise PSD.

- **Computational cost**

  Due to the long duration and the detector motion, CGW searches are quite sensitive to the small difference in the signal parameters. It leads to heavy computational cost.

Glitches

Glitches
= burst-like disturbances

Unlike CBC searches, glitches cannot be the sources of confusion with CGWs.

But, it affects the estimation of PSD by increasing noise floor.

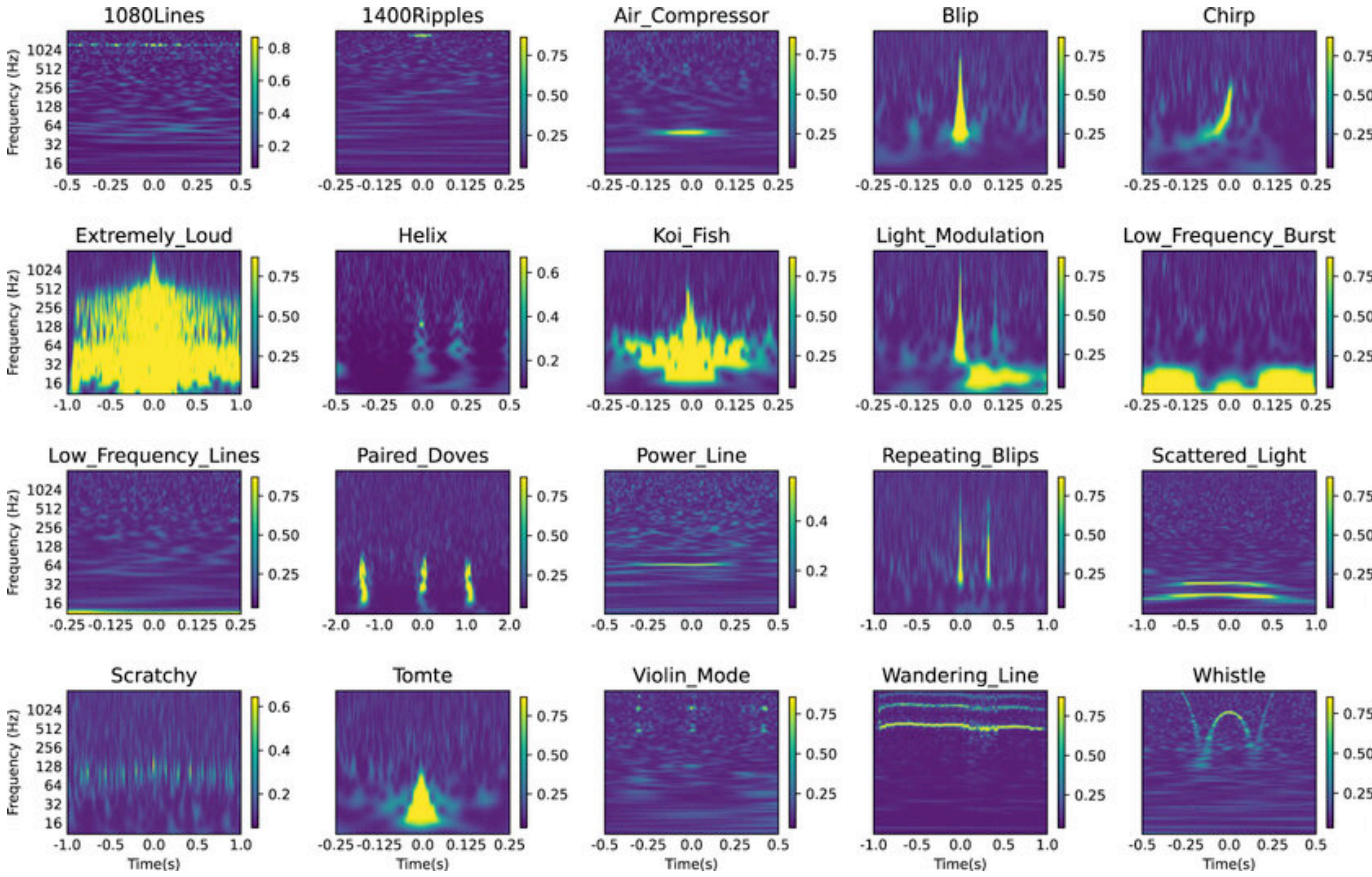

Instrumental lines

Instrumental lines
= narrow band, persistent artifacts

Sources:
- 60Hz power line harmonics,
- Violin modes of suspension
- Environmental disturbances, etc…

Instrumental lines can degrade the CW search sensitivity because they share the similar features with CGWs leading the increase of the false-alarm rate. Also, lines much affect on the PSD estimation.

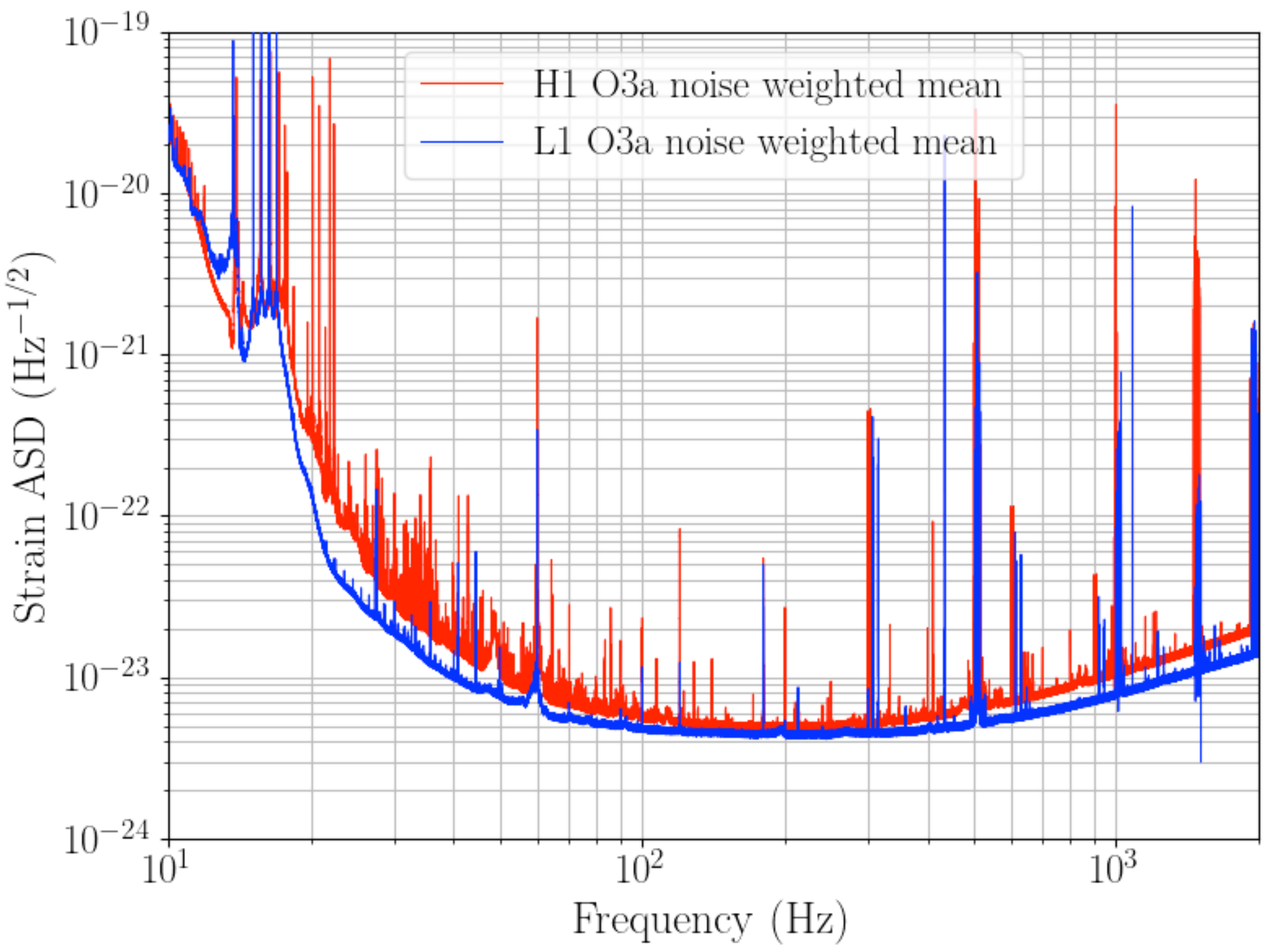

Fig: https://gwosc.org/O3/o3speclines/

$T_{\rm obs}$ dependency of computational cost

Idea: **difference in frequency should be smaller than (T_{obs})$^{-1}$**

Resolutions $\Delta f^{(0)} \sim T_{\rm obs}^{-1}$ $\Delta\alpha \sim \Delta\delta \sim \left(f^{(0)}\frac{v}{c}\right)^{-1} \cdot T_{\rm obs}^{-1}$

$\text{Doppler modulation} \simeq f^{(0)}\frac{\boldsymbol{v}\cdot\boldsymbol{n}}{c}$

$\Delta f^{(1)} \sim T_{\rm obs}^{-2}$

$\text{Small deviation} \sim f^{(0)}\frac{v}{c}\Delta\alpha \lesssim T_{\rm obs}^{-1}$

Volume of the parameter space each grid covers $\Delta V_{\rm grid} \sim (T_{\rm obs})^{-5}$

Computational cost ~ (# of grids) x (comp. cost per grid) ~ $(T_{\rm obs})^6$

Long observational time leads to the rapid increase of the computational cost.

Semi-coherent searches

- Coherently processing entire observational data is not feasible. So, we divide it into short segments, process each segment coherently, and integrate them. Typically, T_{coh} = 1800 sec. But, it can be longer.

- The sensitivity is degraded comparing with the fully-coherent search. But, with the computational resource limitation, semi-coherent searches show better sensitivity than the coherent searches.

- Each algorithm returns candidates which satisfies the criteria and is followed by the follow-up search to confirm whether the candidates are astrophysical signals or detector artifacts.

Various types of CGW search

- The more knowledge we have, the better sensitivity & the more efficient the search is.
- Blind (all-sky) searches are the most expensive task in GW astronomy.
- In this talk, we focus all-sky searches.

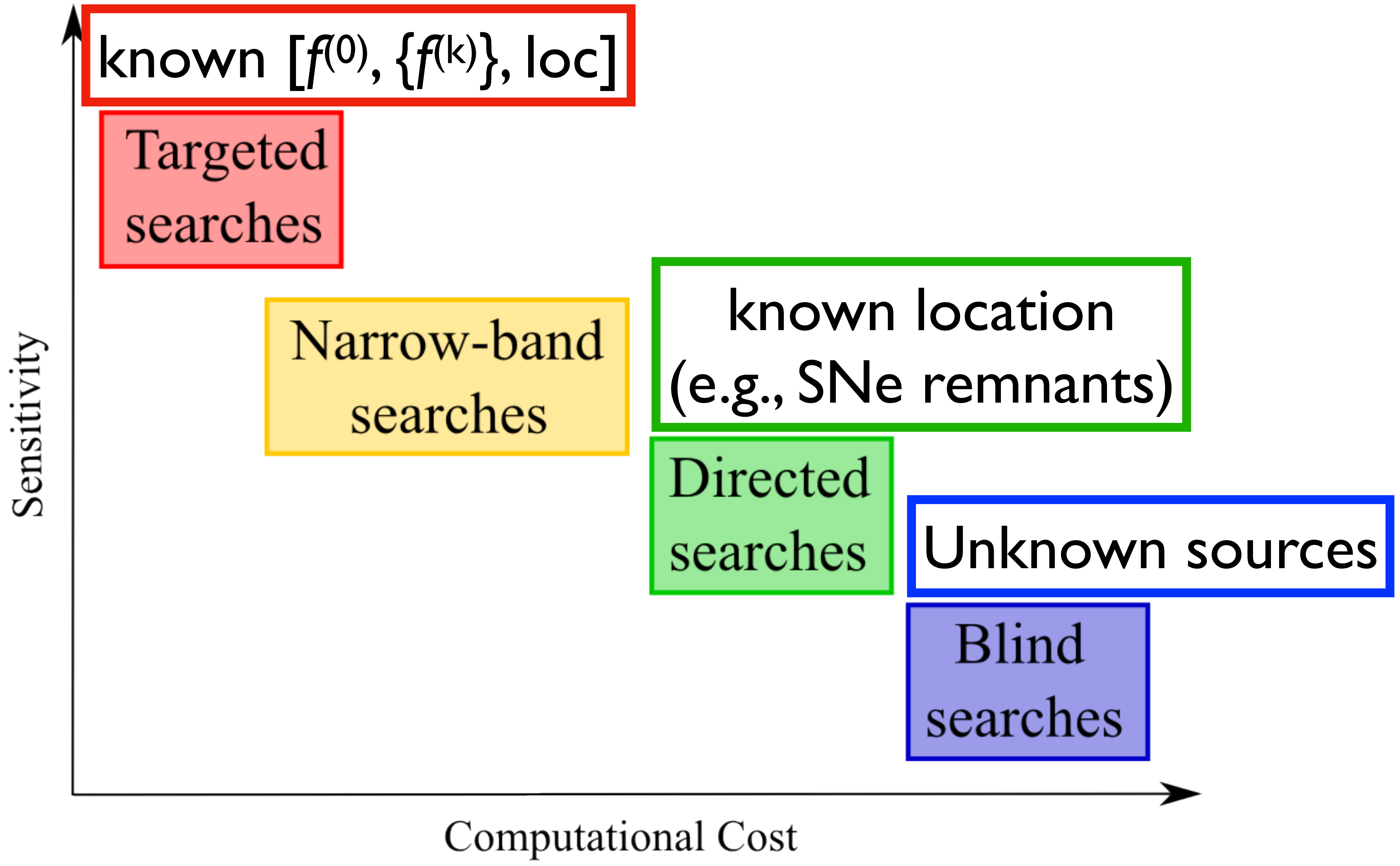

Fig. Sieniawska & Bejger, Universe 5(11), 217 (2019) [modified]

Search pipelines employed in O3 all-sky searches

LVK collaboration, arXiv:2201.00697

- **Time-domain F-statistic**

  Maximum likelihood based approach.

- **Frequency Hough, sky Hough**

  Hough transform. Frequency Hough makes Hough map in ($f^{(0)}$, $f^{(1)}$) plane while sky Hough makes it in (α, δ) plane.

- **PowerFlux**

  Adding SFT powers normalized by noise PSD and antenna pattern functions.

- **SOAP-CNN**

  Combining Viterbi algorithm, machine learning technique to find the likely frequency track, and a convolutional neural network.

Search pipelines employed in O3 all-sky searches

- **Time-domain F-statistic**

  Maximum likelihood based approach.

Hands-on

- **Frequency Hough, sky Hough**

  Hough transform. Frequency Hough makes Hough map in ($f^{(0)}$, $f^{(1)}$) plane while sky Hough makes it in (α, δ) plane.

- **PowerFlux**

  Adding SFT powers normalized by noise PSD and antenna pattern functions.

- **SOAP-CNN**

  Combining Viterbi algorithm, machine learning technique to find the likely frequency track, and a convolutional neural network.

F-statistic

reference

Jaranowski, Królak, and Schutz, Phys.Rev.D58, 063001 (1998)

Matched filter

Notation *s(t)*: strain data, *h(t)*: GW waveform, *n(t)*: detector noise

Assumption: detector noise is stationary and Gaussian with zero mean

Likelihood of *s(t)*

$$P(s|0) \propto \exp\left[-\frac{1}{2}(s|s)\right]$$

In the absence of signal

$$P(s|h) \propto \exp\left[-\frac{1}{2}(s-h|s-h)\right]$$

In the presence of signal

noise-weighted inner product

$$(a|b) = 2\int_{-\infty}^{\infty} \mathrm{d}f\, \frac{\tilde{a}(f)\tilde{b}^*(f)}{S_\mathrm{n}(f)}$$

Log likelihood ratio

$$\ln\Lambda = \ln\frac{P(s|h)}{P(s|0)} = (s|h) - \frac{1}{2}(h|h)$$

noise power spectral density (PSD)

$$\langle\tilde{n}(f)\tilde{n}^*(f')\rangle = \frac{1}{2}S_\mathrm{n}(f)\delta(f-f')$$

Rewrite signal model

- Parameters = { $f^{(0)}$, $\{f^{(k)}\}$, α, δ, h_0, ι, ψ, Φ_0 } 7+s parameters are too heavy.

Frequency evolution Amplitude

$$h(t) = F_+(t;\alpha,\delta,\psi)h_0\frac{1+\cos^2\iota}{2}\cos\left[\Phi(t)+\Phi_0\right] + F_\times(t;\alpha,\delta,\psi)h_0\cos\iota\sin\left[\Phi(t)+\Phi_0\right]$$

Antenna pattern functions

$$F_+(t) = \sin\zeta\left[a(t;\alpha,\delta)\cos(2\psi) + b(t;\alpha,\delta)\sin(2\psi)\right]$$
$$F_\times(t) = \sin\zeta\left[b(t;\alpha,\delta)\cos(2\psi) - a(t;\alpha,\delta)\sin(2\psi)\right]$$

$$h(t) = \sum_{\mu=1}^{4}\mathcal{A}^\mu(h_0,\iota,\psi,\Phi_0)h_\mu(t;f^{(0)},\{f^{(k)}\}\alpha,\delta)$$

F-statistic = likelihood ratio maximized over A^μ

Likelihood ratio can be rewritten by

$$\ln\Lambda = \mathcal{A}^\mu x_\mu - \frac{1}{2}\mathcal{A}^\mu \mathcal{M}_{\mu\nu}\mathcal{A}^\nu \quad \text{with} \quad x_\mu = (s|h_\mu),\ \mathcal{M}_{\mu\nu} = (h_\mu|h_\nu)$$

Easily maximized over $\{A^\mu\}$

Depending only on $\{f^{(0)}, \{f^{(k)}\}, \alpha, \delta\}$

F-statistic

$$2\mathcal{F} := \max_{\mathcal{A}}[\ln\Lambda] = x_\mu \mathcal{M}^{\mu\nu} x_\nu$$

$\mathcal{M}^{\mu\nu}$: inverse matrix of $\mathcal{M}_{\mu\nu}$

Using F-statistic, we can reduce the dimension of the parameter space by 4.

Statistics of F-statistic

F-statistic $2\mathcal{F} = x_\mu \mathcal{M}^{\mu\nu} x_\nu \sim Z_1^2 + Z_2^2 + Z_3^2 + Z_4^2$

In the absence of signal, 2*F* follows χ^2 distribution with 4 d.o.f

$$\mathbb{E}[2\mathcal{F}|0] = 4\,,\ \mathrm{Var}[2\mathcal{F}|0] = 8$$

If signal exists, 2*F* follows non-central χ^2 distribution

with 4 d.o.f and non-centrality of (h|h)

$$\mathbb{E}[2\mathcal{F}|h] = 4 + (h|h)\,,\ \mathrm{Var}[2\mathcal{F}|h] = 8 + 4(h|h)$$

$$\mathrm{SNR} = \frac{\mathbb{E}[2\mathcal{F}|h] - \mathbb{E}[2\mathcal{F}|0]}{\sqrt{\mathrm{Var}[2\mathcal{F}|0]}} = \frac{(h|h)}{2\sqrt{2}}$$

Semi-coherent F-statistc

Divide data into *N* segments and sum all F-statistics over all segments $2\mathcal{F}_{\rm tot} = \sum_{\ell=1}^{N} 2\mathcal{F}_\ell$

In the absence of signal, 2*F* follows χ^2 distribution with 4*N* d.o.f

$$\mathbb{E}[2\mathcal{F}_{\rm tot}|0] = 4N\,,\ \mathrm{Var}[2\mathcal{F}_{\rm tot}|0] = 8N$$

If signal exists, 2*F* follows non-central χ^2 distribution

with 4*N* d.o.f and non-centrality of (h|h)

$$\mathbb{E}[2\mathcal{F}_{\rm tot}|h] = 4N + (h|h)\,,\ \mathrm{Var}[2\mathcal{F}_{\rm tot}|h] = 8N + 4(h|h)$$

$$\mathrm{SNR}_{\rm semi} = \frac{\mathbb{E}[2\mathcal{F}_{\rm tot}|h] - \mathbb{E}[2\mathcal{F}_{\rm tot}|0]}{\sqrt{\mathrm{Var}[2\mathcal{F}_{\rm tot}|0]}} = \frac{(h|h)}{2\sqrt{2N}} = \mathrm{SNR}\cdot\frac{1}{\sqrt{N}}$$

This is an another explanation why semi-coherent search lose sensitivity.

But, under the limit of computational resources, it is not the case.

Frequency Hough

reference

Antonucci *et al.*, Class.Quant.Grav.25:184015,2008 (2008)

Astone *et al.*, Phys.Rev.D90, 042004 (2014)

Peak map

First of all, we make a periodogram and normalize it by noise PSD.

A pixel of the normalized periodogram is classified as a peak if a pixel satisfies two criteria: (1) the power exceeds the given threshold, and (2) it is a local maxima.

Each pixel in a peak map has a value {0, 1}.

(Only noise)

Normalized power

for one SFT segment

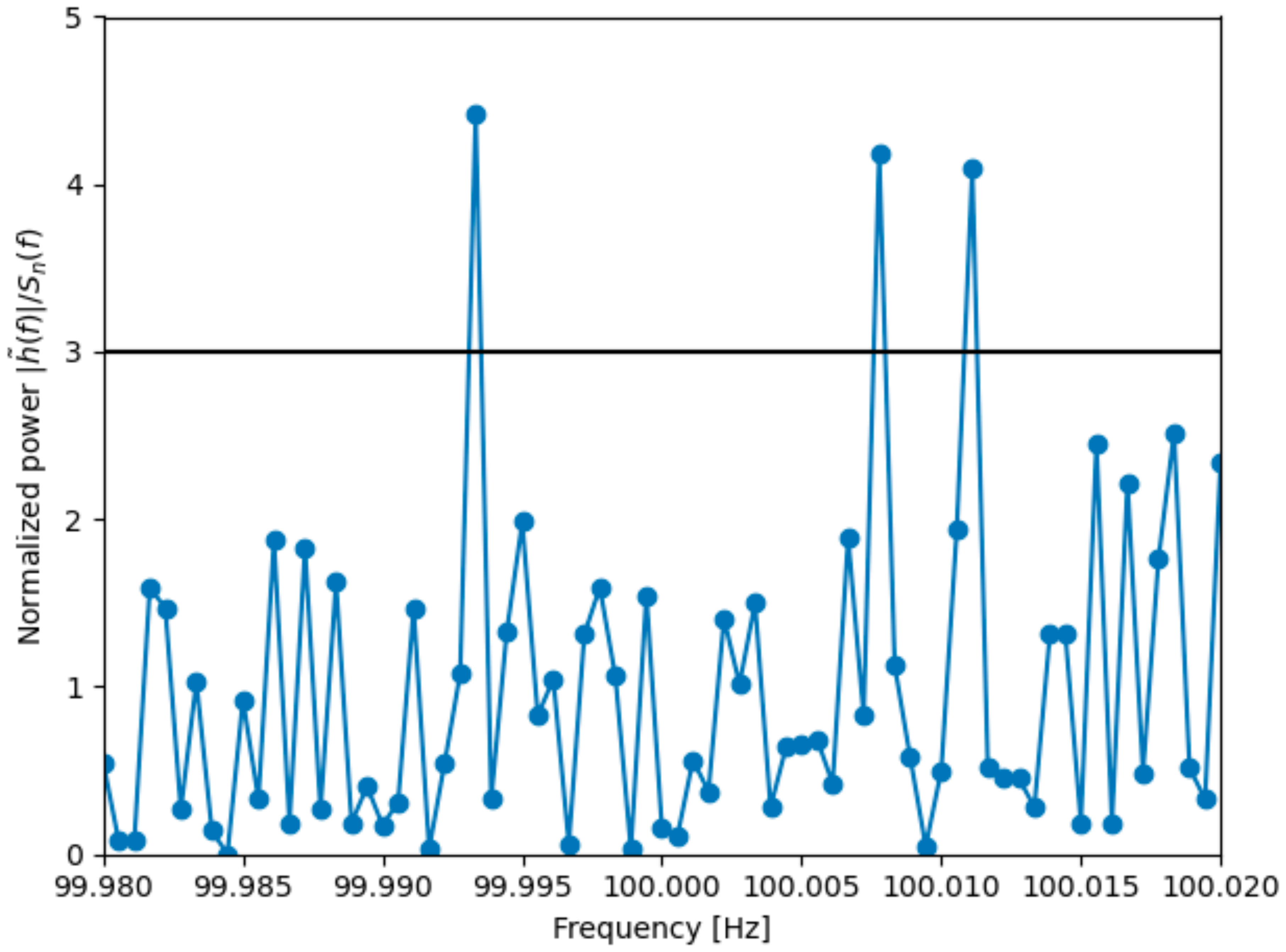

Peak map

Yellow: 1

Purple: 0

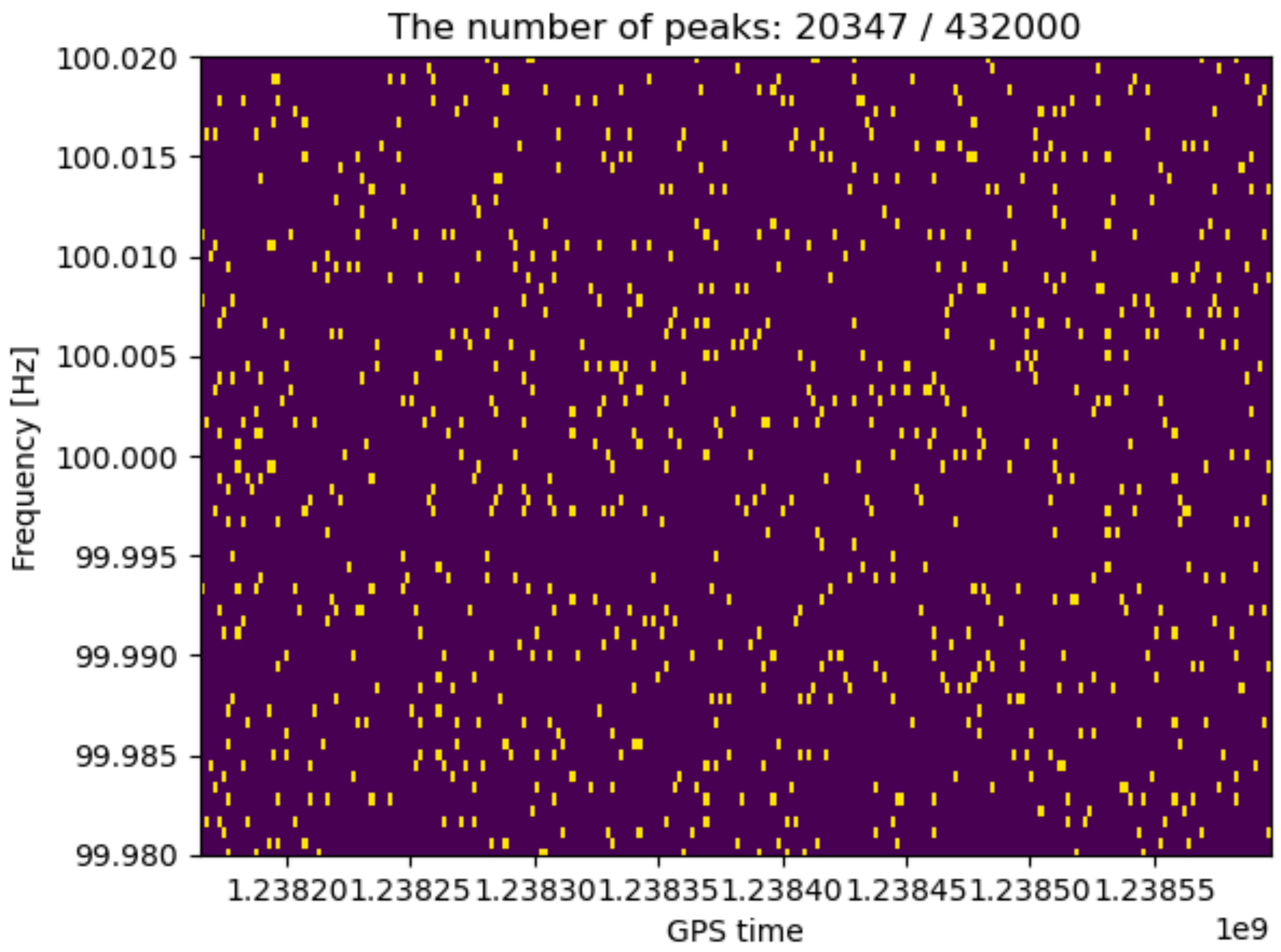

Hough transform

Assuming the relation between the input plane *M* and the parameter space *Σ*,

Hough transform converts each point in *M* into a set of points in *Σ*.

If a point in *Σ* is consistent to a point in *M*, it is incremented by one.

For each grid in *Σ*,

$$\boxed{n = \sum_{i=1}^{N_{\mathrm{SFT}}} n_i \qquad n_i \in \{0, 1\}}$$

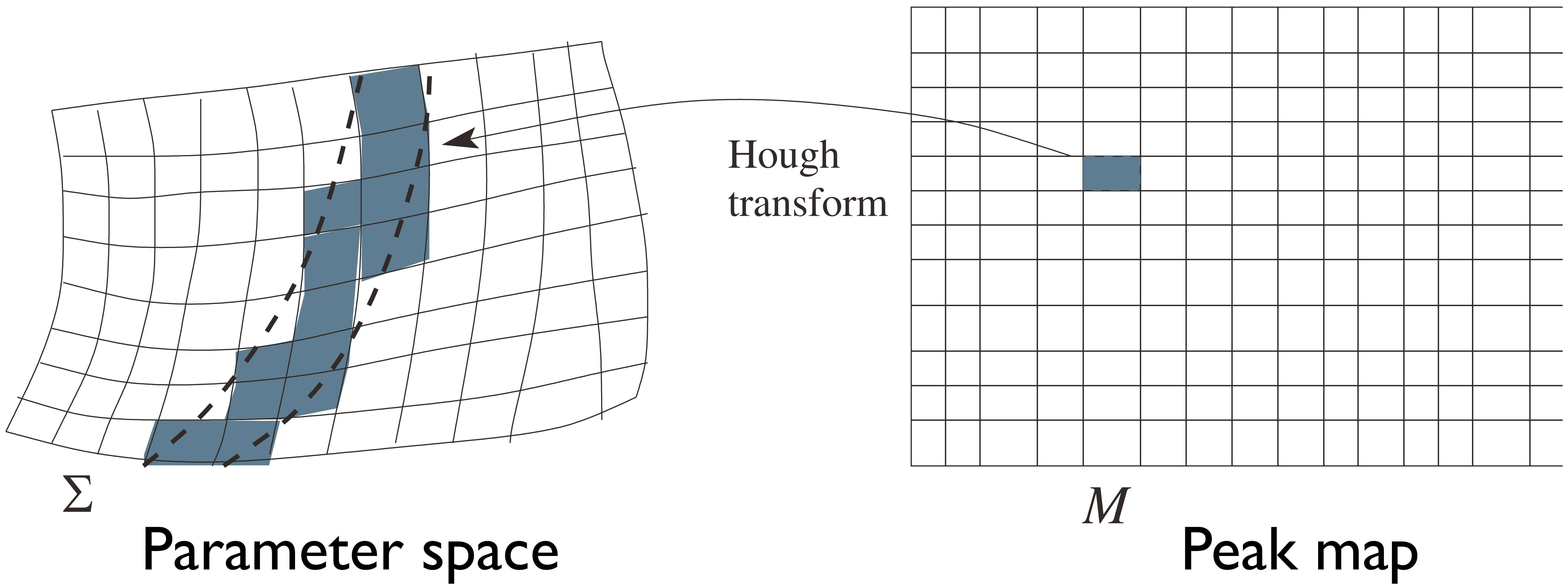

Fig: Krishnan *et al.*, PRD70, 082001

Example: linear function + noise

Data $\{(x_i, y_i)\}$ (i=1,2,…,100), y_i = 1.0 * x_i + 0.5 + n_i, n_i ~ N(0,0.02)

We assume the model $y = a * x + b$ and estimate (a, b).

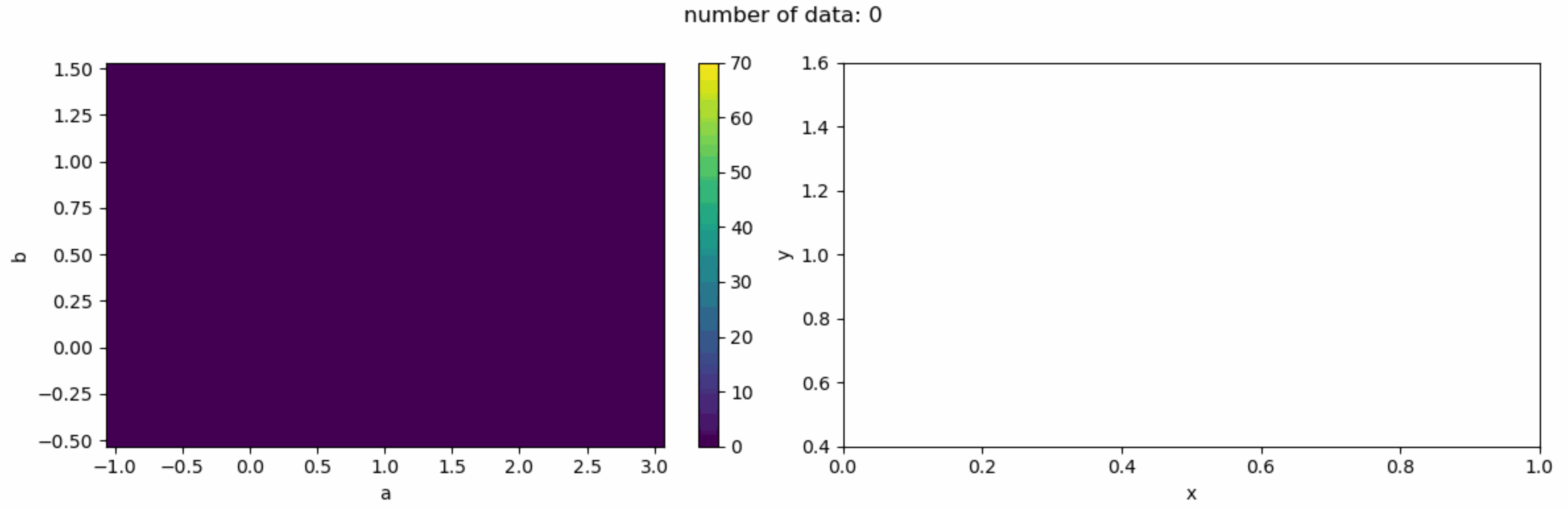

Hough map (parameter space) Input plane

Doppler correction for peak map

For each grid on the sky, we shift the peak map to demodulate the frequency and make a Hough map. Therefore, we have a Hough map for each grid on the sky.

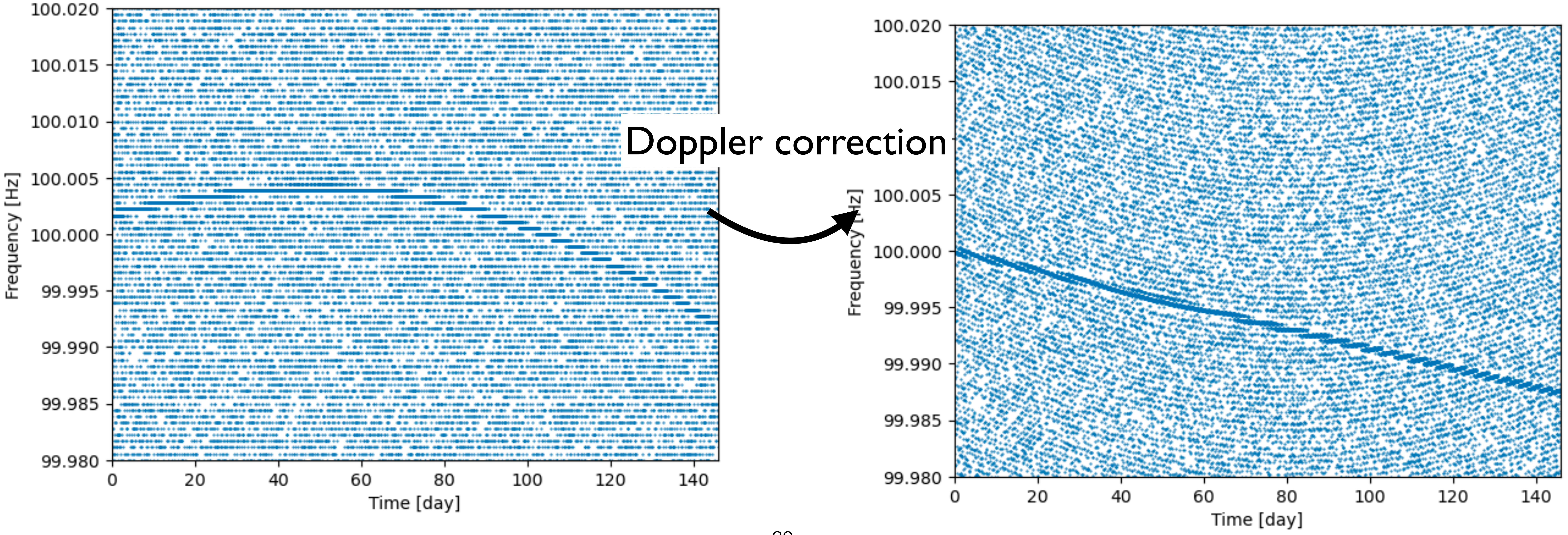

Hough map

Straight line in $(f^{(0)}, f^{(1)})$ plane

After the Doppler correction $f = f^{(0)} + f^{(1)}(t - t_{\rm ref}) \;\Rightarrow\; f^{(1)} = -\dfrac{1}{t - t_{\rm ref}} f^{(0)} + \dfrac{f}{t - t_{\rm ref}}$

Accounting the frequency resolution, each peak is transformed into a stripe in parameter space.

For each grid in Σ,

$$\boxed{n = \sum_{i=1}^{N_{\rm SFT}} n_i \qquad n_i \in \{0, 1\}}$$

Parameter space $(f^{(0)}, f^{(1)})$ Peak map on (t, f)

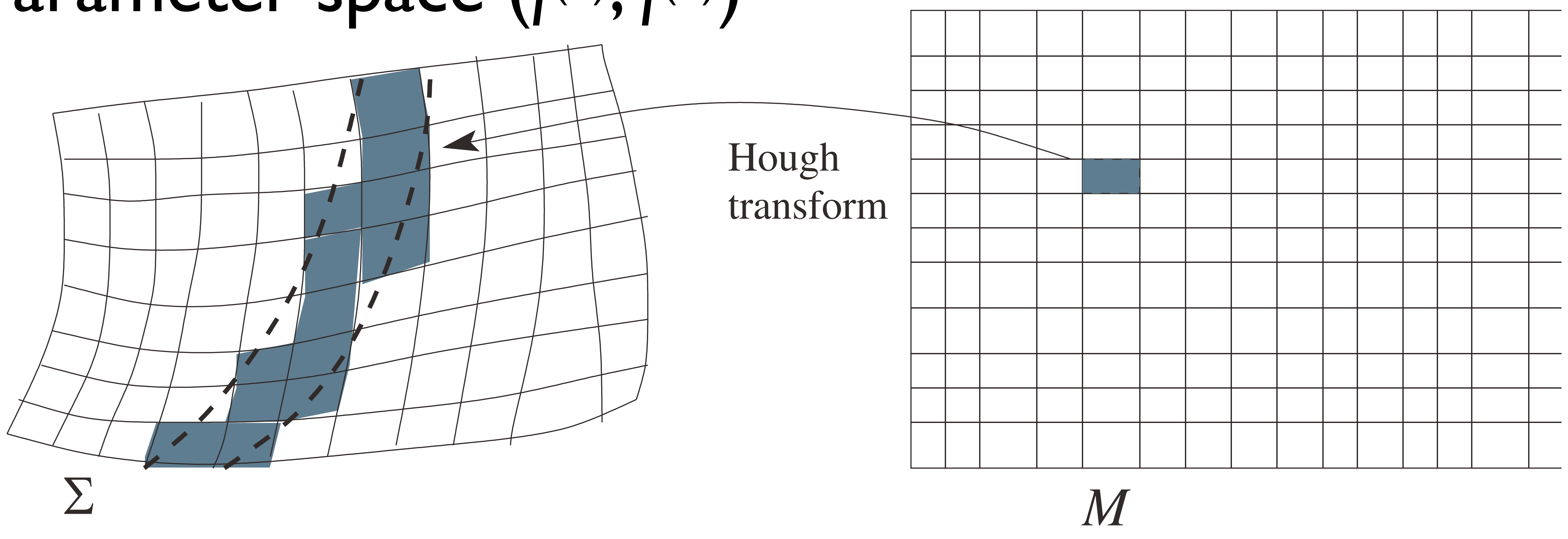

Fig: Krishnan *et al.*, PRD70, 082001

Sum is taken over the frequency track consistent with the grid in Σ.

Calculating n for every grids in Σ, we get a Hough map.

Summary

Summary

- CGWs will provide us with the fruitful information about astrophysics, particle physics, and cosmology.
- Searches for CGWs are challenging due to the computational cost and non-Gaussian noise.
- Various semi-coherent searches are employed to detect CGWs. F-statistic and Hough transform are powerful tools.

I didn’t talk the following:

- Targeted, narrow band, and directed searches
- Sophisticated techniques (grid placement, hierarchical algorithm, etc)
- Pre-processing (gating, line cleaning, making SFT database, etc)
- Post-processing (clustering, coincidence, vetos, etc) and follow-up stage
- Many apps in lalsuite
- Machine learning & deep learning approaches

References

- Review articles (recent)
  - Sieniawska & Bejger, Universe 2019, 5(11), 217 , arXiv: 1909.12600 [CGWs and neutron stars]
  - Tenorio, Keitel & Sintes, Universe 2021, 7(12), 474 , arXiv: 2111.12575 [All-sky searches & post-processing]
  - Piccinni, Galaxies 2022, 10(3), 72 , arXiv: 2202.01088 [Sources and search results including DM candidates]
  - Wette, Astroparticle Physics 153 (2023) 102880 , arXiv: 2305.07106 [Summary of CGW search results]
  - Riles, Living Reviews in Relativity (2023) 26:3 , arXiv: 2206.06447 [Search methods for CGWs]
- Tutorials and slides
  - LIGO India Scientific Collaboration (LISC) workshop, YouTube (Jones (1, 2), Wette, Keitel)
  - PyFstat, https://github.com/PyFstat/PyFstat
  - Tutorial on Frequency Hough by Andrew Miller, https://andrew-l-miller.github.io/post/tutorial/

Backup

ex. Rotating distorted NS

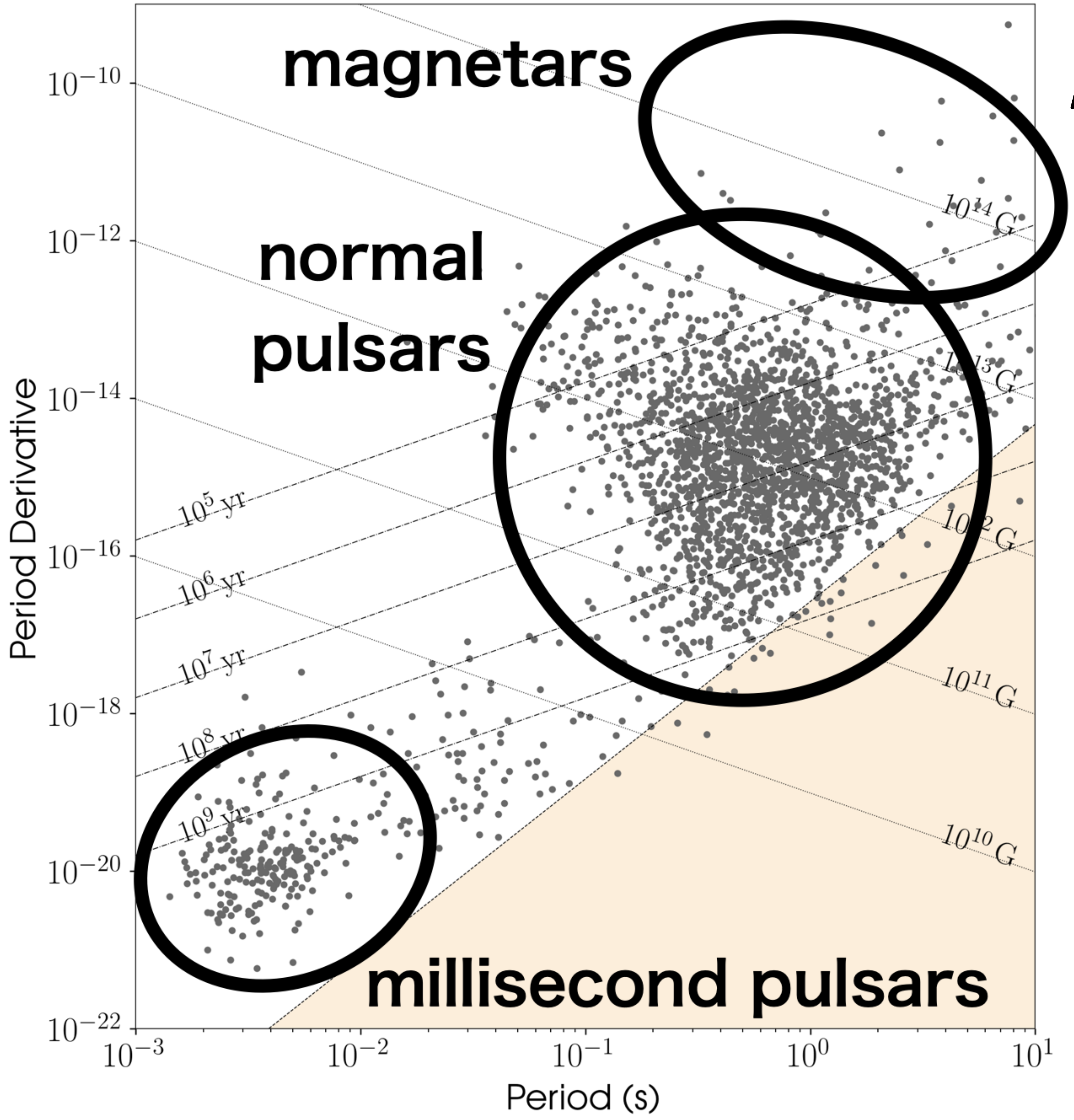

https://www.atnf.csiro.au/research/pulsar/psrcat/

Plotted by `psrqpy`

$$h_0 \simeq 10^{-26} \left(\frac{Q_z}{1.1 \times 10^{45} \text{ g cm}^2} \right) \left(\frac{r}{1\text{kpc}} \right)^{-1} \times \left(\frac{f_{\text{gw}}}{100 \text{ Hz}} \right)^2 \left(\frac{\epsilon}{10^{-6}} \right)$$

ellipticity $\epsilon := \frac{Q_y - Q_x}{Q_z}$

current upper lim. ~ 2 x 10^{-25}

$$\dot{f}_{\text{gw}} \sim f_{\text{gw}}^2 |\dot{P}|$$
$$\sim 10^{-16} \text{ Hz/sec} \left(\frac{|\dot{P}|}{10^{-20} \text{sec/sec}} \right) \left(\frac{f_{\text{gw}}}{10^2 \text{ Hz}} \right)^2$$

ex. Axion clouds around BH

Arvanitaki *et al.*, PRD 81, 123530 (2010)
Brito *et al.*, Class. Quantum Grav. 32, 134001 (2015)

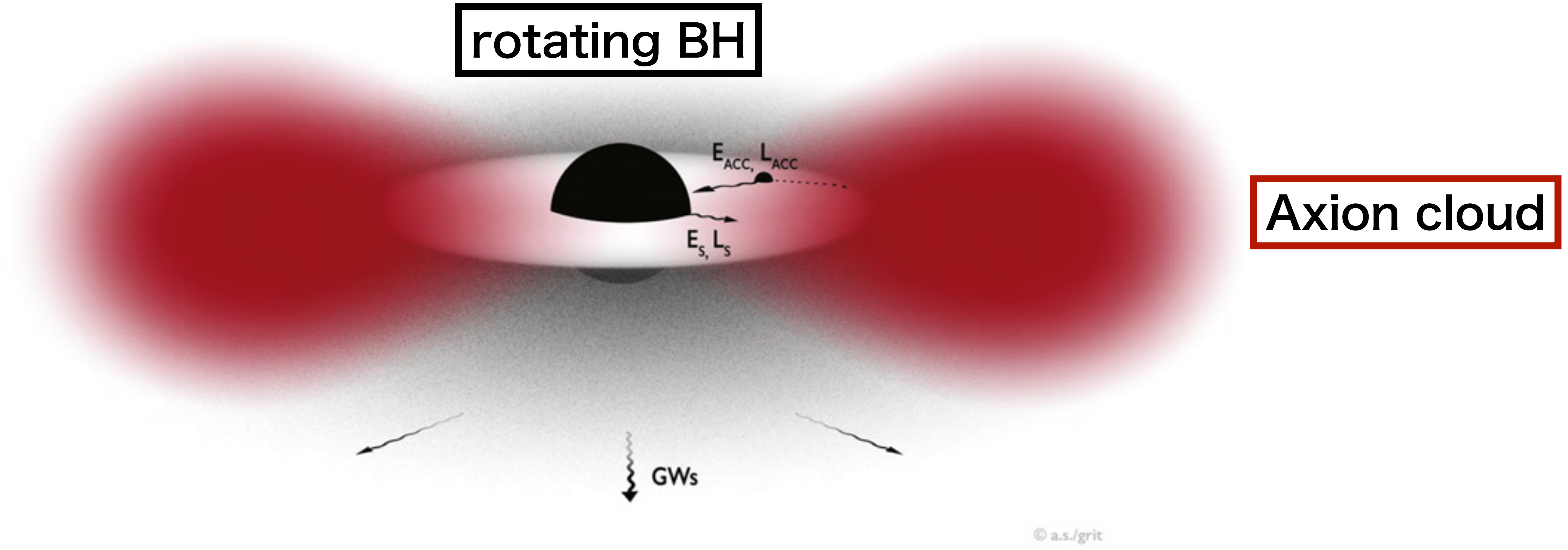

$$h_0 \sim 2.1 \times 10^{-25} \left(\frac{\alpha}{0.075}\right)^7 \left(\frac{M_{\rm BH}}{10 M_\odot}\right) \left(\frac{1{\rm kpc}}{r}\right)$$

$$\alpha := \frac{R_{\rm Sch}}{\lambda_{\rm axion}}$$

$$f_{\rm gw} \sim \frac{2 m_{\rm axion} c^2}{h} \sim 2.5 \times 10^2 \text{ Hz} \left(\frac{m_{\rm axion}}{10^{-12} \text{ eV}}\right)$$

$$\tau_{\rm GW} \sim \frac{M_{\rm cloud} c^2}{\mathcal{L}_{\rm GW}} \sim 1.9 \times 10^{11} \text{ sec} \left(\frac{\alpha}{0.075}\right)^{-15} \left(\frac{M_{\rm BH}}{10 M_\odot}\right)$$

Sasaki *et al.*, Class. Quantum Grav. 35, 063001 (2018) as a review of PBH

ex. Small mass PBH binaries

of PBHs in our Galaxy (assuming DM consists of PBHs)

$$M_{\rm DM} \sim 1.7 \times 10^{15} M_\odot \left(\frac{R}{3{\rm Mpc}}\right)\left(\frac{v}{1500{\rm km/s}}\right)$$

$$N_{\rm PBH} \lesssim \frac{f_{\rm PBH} M_{\rm DM}}{m_{\rm PBH}} \sim 1.7 \times 10^{20} \left(\frac{m_{\rm PBH}}{10^{-6} M_\odot}\right)^{-1}$$

$$n_{\rm PBH} \lesssim \frac{N_{\rm PBH}}{R^3} \sim 6{\rm pc}^{-3}$$

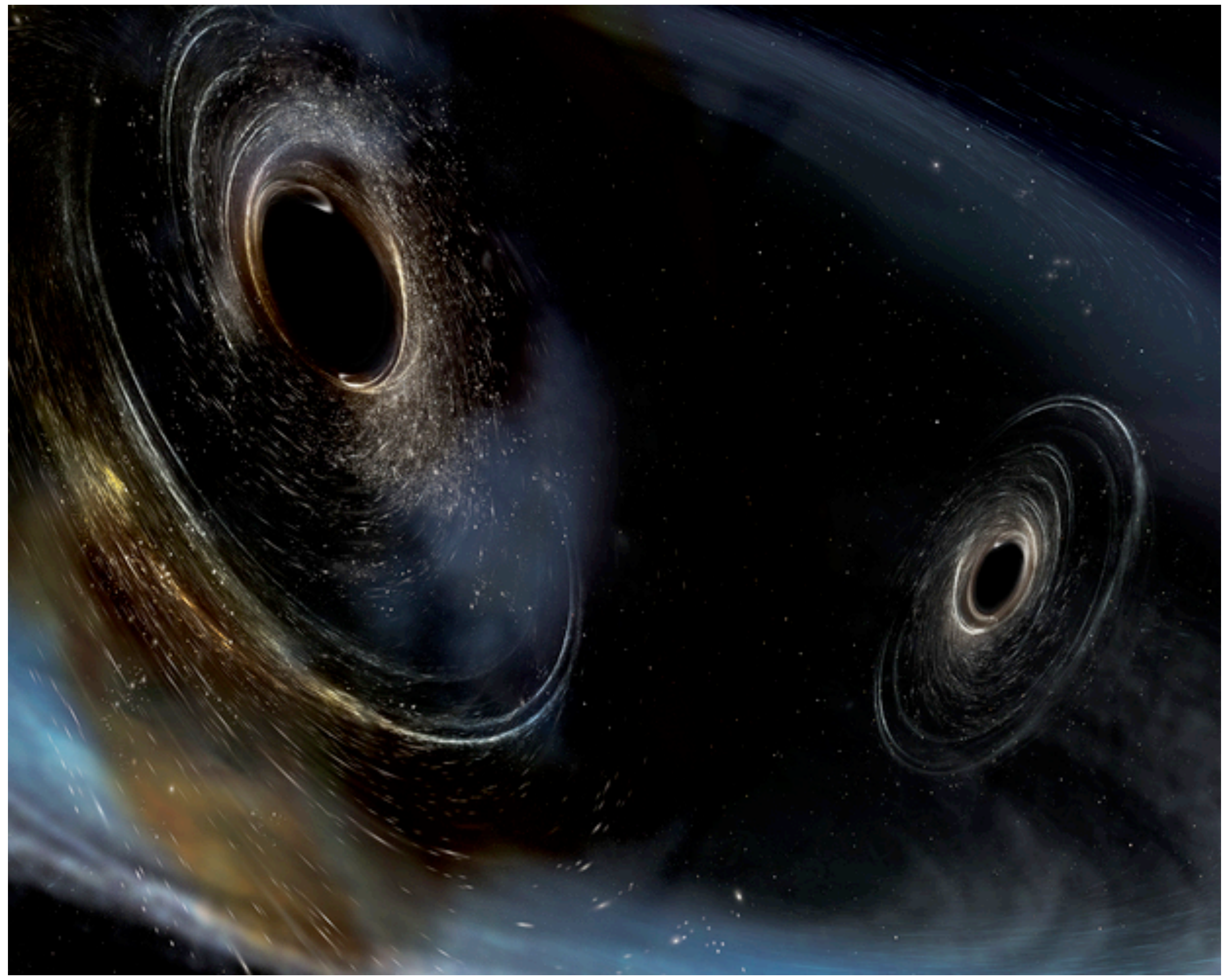

Fig: LIGO

if PBHs form a binary,

$$h_0 \sim 2 \times 10^{-25} \left(\frac{\mathcal{M}_{\rm c}}{10^{-6} M_\odot}\right)^{5/3} \left(\frac{f_{\rm gw}}{100{\rm Hz}}\right)^{2/3} \left(\frac{r}{1{\rm pc}}\right)^{-1}$$

$$\dot{f}_{\rm gw} \sim 10^{-9}\ {\rm Hz/\,sec} \left(\frac{\mathcal{M}_{\rm c}}{10^{-6} M_\odot}\right)^{5/3} \left(\frac{f_{\rm gw}}{100\ {\rm Hz}}\right)^{11/3}$$